Stearic Acid Spin Labels in Lipid Bilayers: Insight through Atomistic Simulations

ARTICLE *in* THE JOURNAL OF PHYSICAL CHEMISTRY B · DECEMBER 2007

Impact Factor: 3.3 · DOI: 10.1021/jp0746796 · Source: PubMed

Stearic Acid Spin Labels in Lipid Bilayers: Insight through Atomistic Simulations

Lorna Stimson,[†,‡] Lei Dong,[†] Mikko Karttunen,[‡] Anna Wisniewska,[§] Małgorzata Dutka,[§] and Tomasz Róg*[,§,||]

Laboratory of Physics, Helsinki University of Technology, Finland, Department of Applied Mathematics, The University of Western Ontario, London (ON), Canada, Department of Biophysics, Faculty of Biochemistry, Biophysics and Biotechnology, Jagiellonian University, Kraków, Poland, and Biophysics and Statistical Mechanics Group, Department of Electrical and Communication Engineering, Helsinki University of Technology, Finland

Received: June 16, 2007; In Final Form: July 31, 2007

Spin-labeled stearic acid species are commonly used for electron paramagnetic resonance (EPR) studies of cell membranes to investigate phase transitions, fluidity, and other physical properties. In this paper, we use large-scale molecular dynamics simulations to investigate the position and behavior of nitroxide spin labels attached to stearic acid molecules in dipalmitoylphosphatidylcholine (DPPC) bilayers. The results of these studies are potentially very important for the interpretation of EPR spectra, which rely on assumptions about the position of the label in the membrane. Additionally, we investigate the effect of chirality and ionization of the carboxyl group of the label. For a non-ionized species, we observe that spin-label molecules are even able to make flip-flop transitions between the leaflets of the bilayer. Such transitions have been previously observed only in very rare cases in molecular simulations.

Introduction

Several spectroscopic methods can be used to investigate the structure and dynamics of biological and model membranes. The most common techniques are ^{2}H NMR, ^{13}C NMR, Raman, infrared, fluorescence, and electron paramagnetic resonance (EPR) spectroscopy. As all of these methods have their advantages and disadvantages and probe different properties; they are considered to be complementary. The EPR spin-labeling technique, the focus of this study, has been used for many years to obtain information about the physical properties of membranes, such as fluidity, polarity, permeability to polar and nonpolar molecules, oxygen and nitric oxide transport, and lipid phase transitions.[1−5]

Spin labels are usually stable nitroxide free radicals, which give characteristic EPR spectra.[6] The three-line pattern of the spectrum reflects the hyperfine interaction, which for membrane systems is anisotropic and may vary with the orientation of the magnetic field relative to the nitroxide axes.[6] Different types of nitroxide spin labels are used for labeling in cell membranes. The most common ones are stearic acid derivatives with an oxazolidine ring, where the nitroxide group is flanked by quaternary carbon atoms. The oxazolidine ring can be attached to various carbons in the stearic acid chain. The motion of the nitroxide reflects the motion of the labeled part of the molecule, which in turn provides information about the local environment at a given depth in the membrane.

For EPR spectra interpretation, it is usual to assume that a position of the nitroxide group in the stearic acid chain remains constant and is the same as its position relative to the host phospholipid. On the basis of that assumption, the profiles of different physical properties across the membrane have been obtained, such as the oxygen transport parameter, polarity, and order parameters.[2,3,7] The oxygen transport parameter profile is very useful for the characterization of the membrane dynamics and structure in the third dimension, that is, normal to the plane of the membrane.[8] In this approach, the rate of collision between molecular oxygen and the nitroxide moiety attached to a specific location in the lipid is measured using the pulse EPR method.[8] Molecular oxygen, due to its small size and appropriate level of hydrophobicity, is able to enter small vacant pockets that are transiently formed in the lipid bilayer. Therefore, the collision rates between molecular oxygen and nitroxide spin labels at specific locations in the membrane are sensitive to the dynamics of gauche−trans isomerization of lipid hydrocarbon chains and to the structural non-conformability of neighboring lipids.[7,9,10] This method provides unique information about the three-dimensional structure and dynamics of lipid membranes, and it is also unique in characterizing membrane domains without the need for their separation.[8] However, vertical fluctuations of the nitroxide moiety of spin labels toward the surface of the membrane have been reported based on bimolecular collision rates between nitroxide moieties at different locations along the acyl chain[11,12] and also between 8-anilinonaphthalene-1-sulfonic acid (ANS) and nitroxide moieties.[13]

It is accepted that the presence of low concentrations of a stearic acid spin label (SASL) in a membrane has a negligible perturbation effect. However, this is not necessarily the case. Previously, we have studied the effect of placing the bulky oxazolidine ring in the dimyristoylphosphatidylcholine (DMPC) membrane on the DMPC main phase transition.[4] The effect manifests itself by lowering the main phase transition temperature of DMPC. This effect was strongest for the spin label

* Author to whom correspondence should be addressed. E-mail: tomasz.rog@gmail.com. Web: www.softsimu.org.
[†] Laboratory of Physics, Helsinki University of Technology.
[‡] The University of Western Ontario.
[§] Jagiellonian University.
[||] Department of Electrical and Communication Engineering, Helsinki University of Technology.

10.1021/jp0746796 CCC: $37.00
Published on Web 10/11/2007

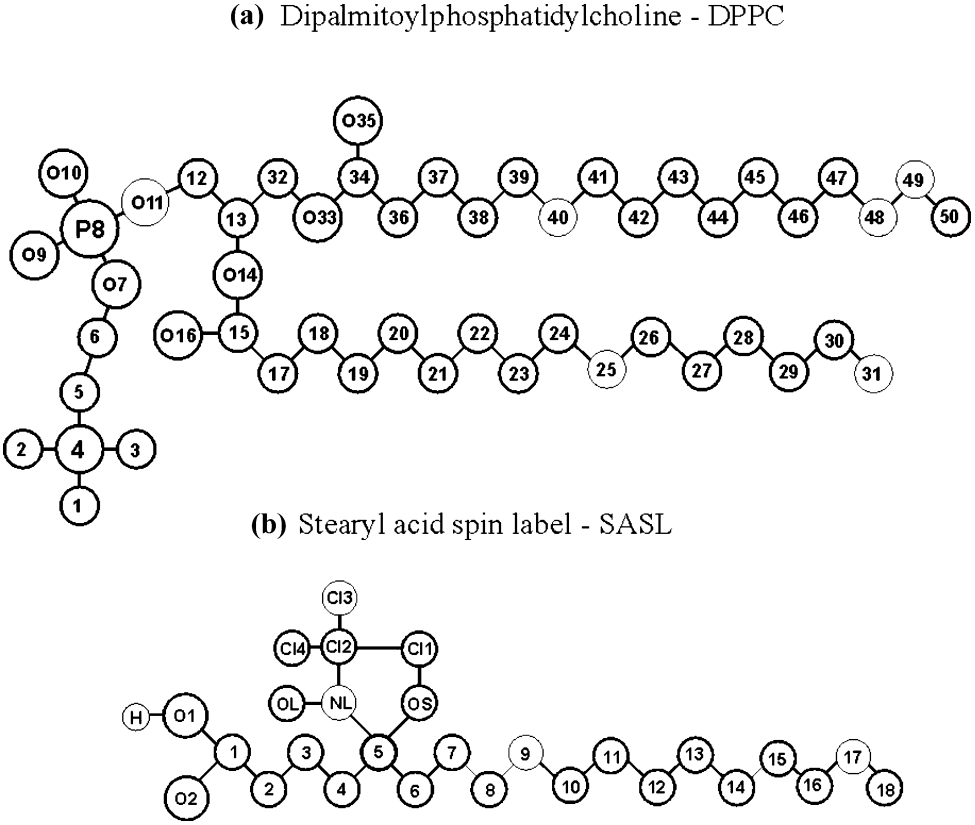

Figure 1. Molecular structures of (a) DPPC, and (b) SASL molecules with numbering of atoms. (Labeled at the 5th position.)

with a nitroxide group at the 9th position (9-SASL, in the middle of the acyl chain), and weakest for the spin label with a nitroxide group at the 16th position (16-SASL, close to the terminal methyl group). The highest SASL concentration used for EPR measurements was 3 mol %; however, the effect of 9-SASL was considerable with a label concentration as low as 1 mol %.[4] It has been concluded that the perturbing effect was caused by packing defects arising in the gel phase. Recent molecular dynamics (MD) simulations of spin-labeled perifosine (which is a drug candidate) in a dipalmitoylphosphatidylcholine (DPPC) membrane showed that the position, size, and hydrophilicity of the doxyl group perturbed the overall lipophilic nature of the compound as well as the anchoring properties of the acyl chain.[14]

In this paper, we used MD simulations to study lipid bilayers containing SASL molecules with a label attached at the 5th, 10th, or 16th carbon atom along the chain. The problem of the effect of spin labeling on macromolecular structures using MD has been the subject of a few recent papers, mainly concerning the effect of labels on protein structure.[15−17] To our knowledge, only three papers have described the behavior of labels in membrane systems. Håkansson et al. concentrated on calculations of EPR spectra from trajectories of spin labels inserted into lipid bilayers,[18] Mravljak et al. studied label conformations in lipid bilayers,[14] and Sammalkorpi and Lazaridis simulated interactions of spin-labeled fusion peptides with lipid bilayers.[19] Here, we concentrate on structural and dynamical properties of lipid bilayers with incorporated SASL molecules to provide data useful for the interpretation of experimental results. In particular, we analyze the location of labels in a bilayer, their rotations, and electrostatic interactions with the lipid molecules and water. The effect of the presence of labels on bilayer properties is also discussed.

Methods

System Description and Parameters. Atomic-scale MD simulations have been performed on five different membrane systems. Each bilayer was composed of a matrix of 128 DPPC molecules with 16 (11 mol %) SASL molecules regularly inserted among the DPPC. We used three types of SASL molecules with labels attached in an *R* configuration to carbons 5, 10, and 16, which we denote as 5r, 10r, and 16r, respectively. Additionally 5-SASL, in an *S* configuration at C5 (5s), and in a neutral non-ionized form in an *R* configuration (5rh) were constructed. All five bilayers were hydrated with 3500 water molecules. For charged systems, Na^+ counterions were added to preserve the overall charge neutrality of the system. The initial structures of all bilayers were obtained by arranging the DPPC molecules in a regular array in the bilayer (x, y) plane with an initial surface area of 0.64 nm^2 per DPPC molecule.[20] An equal number of label molecules were inserted into each leaflet. Prior to MD simulations, the steepest-descent algorithm was used to minimize the energy of the initial structure.[20,21] The studies were performed using the GROMACS software package.[22] The MD simulations of all bilayer systems were carried out over 120 ns. The first 20 ns were considered to be an equilibration period,[23] and thus only the last 100 ns of the trajectory were analyzed. The approach to equilibrium state was judged by monitoring the membrane surface area which achieved a constant value after less than 5 ns of simulation. Figure 1 shows the structure and atom numbering of DPPC and SASL molecules. A pure DPPC bilayer was used as a reference system.[24]

The well-established and extensively used standard united atom force-field parameters were used for DPPC,[25] where the partial charges were taken from the underlying model description.[26] For water, we employed the simple point-charge (SPC) model.[27] The Na^+ counterions were modeled using the GRO-

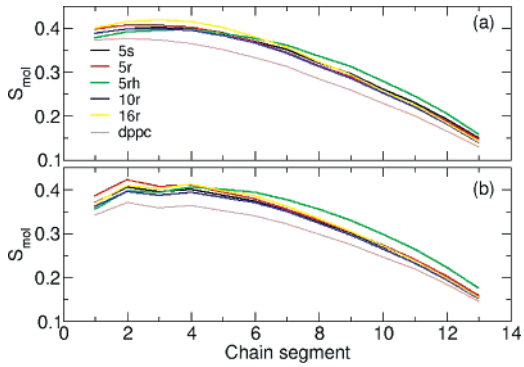

Figure 2. Profiles of the molecular order parameter (S_{mol}) calculated for (a) the DPPC *sn*-1 and (b) *sn*-2 chain.

MACS parametrization which has been shown to work well with the SPC water model.[28] For the SASL molecule acyl tails, we used the same force-field parameters as for DPPC, supplementing them with charges on the carboxyl group from the standard GROMACS set. The nitroxide group was parametrized with parameters derived specifically for nitroxide system simulations by means of ab initio calculations by Barone and co-workers.[29]

Periodic boundary conditions with the usual minimum image convention were used in all three directions. The LINCS algorithm[30] was used to preserve the hydrogen-bond lengths. The time step was set to 2 fs, and the simulations were carried out at constant temperature and pressure using the Berendsen method[31] with relaxation times set to 0.6 and 1.0 ps, respectively. A pressure of 1 atm and a temperature of 323 K, which is above the main phase transition for DPPC,[32] were used. The temperatures of the solute and solvent were controlled independently. The pressure was controlled semi-isotropically, and the Lennard-Jones interactions were cut off at 1.0 nm. For the electrostatic interactions, we employed the particle-mesh Ewald (PME) method[33] with a real space cutoff of 1.0 nm, β spline interpolation (of order 5), and direct sum tolerance of 10^{-6}. It has been shown that PME is a very reliable method in reproducing the correct static and dynamic properties in membrane simulations.[21,34] The simulation protocol used in this study has been successfully applied in various MD simulation studies of lipid bilayers.[21,23,24,33] Errors were estimated following the block analysis method described in ref 35.

Results

Effect of the Labels on the Membrane Structure. To monitor the effect of label molecules on bilayer properties, the molecular order parameter S_{mol}[36] and surface area per chain were calculated in mixed DPPC−label bilayers and compared with those obtained for the pure bilayer. The order parameter for the *n*th segment of an acyl chain, S_{mol}, was calculated using

$$S_{mol} = \frac{1}{2}\langle 3\cos^2\theta_n - 1\rangle$$

where θ_n is an instantaneous angle between the *n*th segmental vector, that is, (C_{n-1}, C_{n+1}) vector linking $n-1$ and $n+1$ carbon atoms in the acyl chain and the bilayer normal; $\langle\ \rangle$ denotes the time average (and by ergodicity, the ensemble average). Profiles of the order parameter S_{mol} are shown in Figure 2. The average values of S_{mol} over the chain and the surface area per chain are given in Table 1. These parameters are the two most informative ones about the membrane structure. As can be seen from Figure 2 and Table 1, the effect of spin labels on membrane properties is small and for most systems is within the error range. Figure 3 shows the density profiles of DPPC, the label, and water. These profiles are typical for lipid bilayers.[21] Snapshots of the equilibrated structures of 5r and 16r systems are shown in Figure 4.

TABLE 1: Average Values of the Molecular Order Parameter, S_{mol}, and Average Surface Area per Chain[a,b]

membrane	S_{mol} *sn*-1	S_{mol} *sn*-2	area [nm^2]
5r	0.32 ± 0.01	0.32 ± 0.01	0.322 ± 0.001
5rh	0.33 ± 0.01	0.32 ± 0.01	0.321 ± 0.002
5s	0.34 ± 0.01	0.32 ± 0.01	0.324 ± 0.002
10r	0.32 ± 0.01	0.31 ± 0.01	0.323 ± 0.001
16r	0.33 ± 0.01	0.32 ± 0.01	0.325 ± 0.001
DPPC	0.29 ± 0.01	0.28 ± 0.01	0.330

[a] For the area per chain, the error estimates have been made by calculating block averages, then extrapolating to large block sizes. [b] Standard errors have been calculated for S_{mol}.

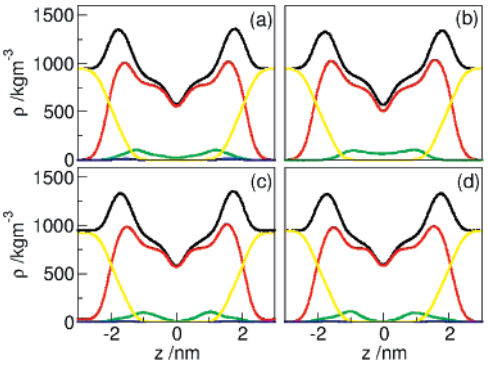

Figure 3. Partial density profiles along the bilayer normal in (a) 5r, (b) 5rh, (c) 10r, and (d) 16r system; red line: DPPC atoms, green line: SASL atoms, yellow line: water atoms, black line: all atoms in the system. The coordinate $z = 0$ corresponds to the membrane center.

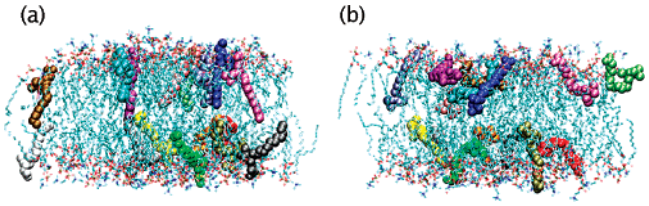

Figure 4. Snapshots showing equilibrated structure of 5r and 16r systems.

Location of Labels. *Effect of Label Position*. The partial density profiles along the bilayer normal for the SASL C1 carbon atom, NL and OL atoms, all label ring atoms, and each DPPC *sn*-1 tail carbon atoms were calculated. These are shown for the 5r and 16r systems in Figure 5a,b to illustrate the dependence of the location of the labels in the bilayer on its position along the acyl chain. Additionally, in Figure 5c the density profiles of NL and OL atoms in all systems are shown. To demonstrate the precise location of the labels with respect to DPPC chains, Figure 6 shows the average locations of DPPC acyl chain atoms along the bilayer normal and the average position of a label. The error bars shown in Figure 6 represent the standard deviation calculated from the time average of the density profiles of the respective atoms and therefore illustrate the width of the distribution rather than the accuracy of the simulations.

As can be seen from Figure 6, the position of the label on the SASL tail is shifted relative to the position of DPPC atom tails; 5r is located at the position of C3−C4, 10r at C6, and 16r at C8−C9. This indicates that the average position of labels on

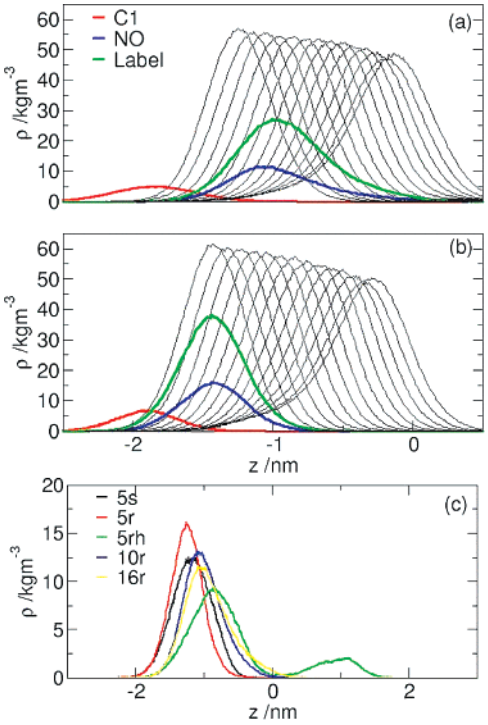

Figure 5. Density profiles of SASL C1 (red line) atom, OL and NL atoms (blue line), all label ring atoms (green line), and DPPC *sn*-1 tails atoms, each carbon atom separately (black lines, first curve is for C31 and other curves for carbon atoms of the tail in order) in the 16r (a) and 5r (b) system; density profiles of OL and NL atoms in all studied systems (c).

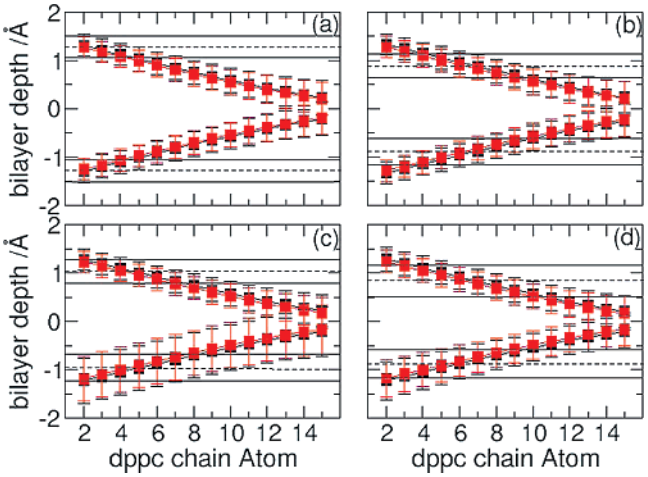

Figure 6. Average position along bilayer normal of DPPC acyl chains atoms (black represents *sn*-1 and red *sn*-2 chain) and position of SASL OL atom (dashed horizontal line; the solid horizontal line represents the standard deviation ranges of the average position) in (a) 5r, (b) 5rh, (c) 10r, and (d) 16r systems.

the SASL carbon chain does not directly correspond to that of DPPC, but that there is a larger shift for larger indexes.

Effect of Chirality. Partial density profiles along the bilayer normal of NL and OL atoms in 5r and 5s SASL molecules, shown in Figure 5c, illustrate the effect of the label chirality on its location in the membrane. Figure 5c shows a slightly deeper location for the nitroxide bond with the *S* enantiomer. The difference between the average positions is 0.2 nm.

Effect of Ionization. Comparison of the partial density profiles of NL and OL atoms in 5r and 5rh SASL molecules along the bilayer normal, shown also in Figure 5c, illustrates the effect of the label ionization on its location in the membrane. The

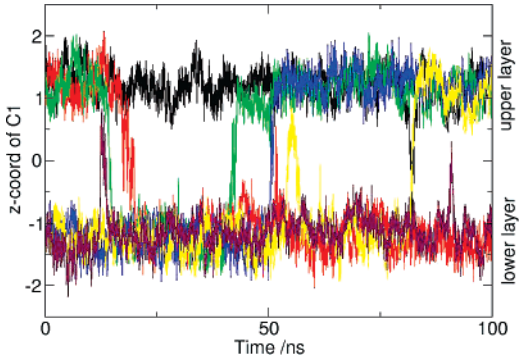

Figure 7. Trajectories of *Z* coordinate (along the bilayer normal) of the SASL C1 atom in the 5rh system.

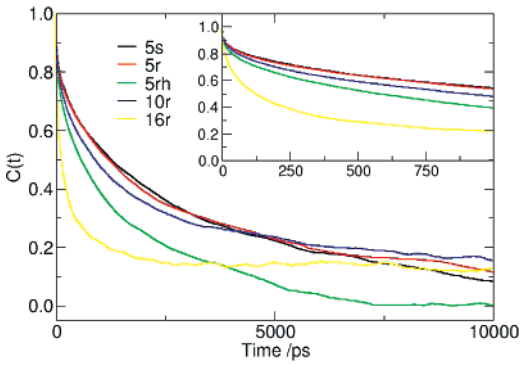

Figure 8. Reorientational autocorrelation function (*C*(*t*)) for the NL-OL vector. Inset to the figure shows the same data for a shorter time scale.

average locations of DPPC acyl chain atoms along the bilayer normal and the average position of the label are shown in Figure 6. Non-ionized labels are located much deeper in the membrane core at about 0.8 nm from the interface, which is approximately the position of DPPC tail atoms C6−C7.

In Figure 7, the trajectories of the positions of carboxyl groups of 5rh SASL are shown. Some SASL molecules are observed flipping between the two membrane layers. We observed three effective inter-leaflet transitions, that is, flip-flops, where the label remained in the opposite layer for more than 1 ns and about 6 ineffective attempts where the carboxyl group of a label entered the opposite leaflet briefly. In the same time period, no such flip-flops were observed for SASL molecules in the ionized forms (5r, 10r, 16r, and 5s). For such transitions, the 5rh SASL molecules first move toward the center of the membrane, their orientations fluctuating strongly. Then, from an almost horizontal orientation it is possible for the SASL molecules to either return to the original leaflet or move to the opposite leaflet.

Rotational Motions of Labels. Reorientational autocorrelation functions (RAF) calculated for the OL-NL vector in SASL molecules are shown in Figure 8. The fastest rotation rate is for the labels attached at the ends of the acyl chains and slower for labels attached at their beginning. This result is in agreement with experimental data.[1,37] As can be seen from the inset in the Figure 8, there is no difference between rotations of 5r and 5s molecules during the first nanosecond, such differences occur on the longer time scale and probably result from a lack of accuracy.

None of the curves for deprotonated systems decay to zero. This is indicative of restricted or anisotropic rotation. Results of experimental investigations using EPR spectroscopy[37] have been consistently explained assuming restricted rotational motion of the spin label around the membrane director. This can be

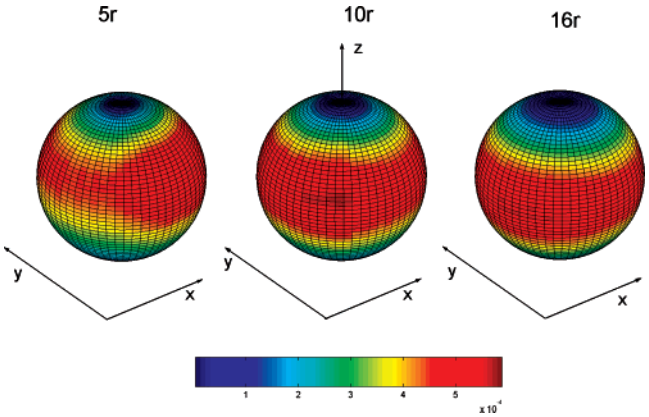

Figure 9. Distribution of the polar angles (Θ,φ) of the vector representing the π-orbital projected on the sphere. Color scale: blue indicates low probability, red indicates high probability. Z: bilayer normal, XY: bilayer plane.

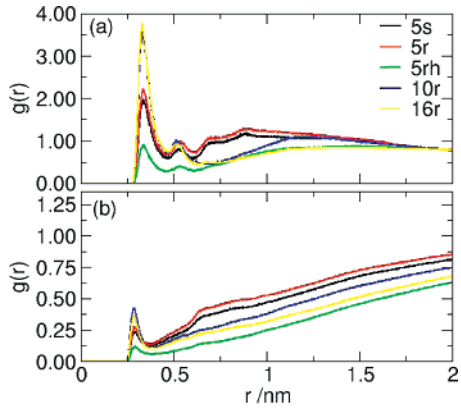

Figure 10. Radial distribution functions ($g(r)$) calculated for the SASL atom OL relative to DPPC choline methyl groups (a) and water oxygen (b).

described by an orientation of the vector representing the π-orbital direction (z_π) with respect to the membrane director (Θ angle, within $<0,\pi>$), and in the perpendicular plane with respect to x_{lab} direction (φ angle, within $<0,2\pi>$). To illustrate this, we calculated the distribution of z_π adopted orientations. The distribution is presented in the form of a sphere where each point on the sphere represents the available polar angles (Θ,φ), and the probability is color-coded (Figure 9). This shows that the distribution is anisotropic for all three labels and is the most pronounced for the 5r spin label.

Polar Interactions of Labels. The NL and OL atoms of the spin labels are relatively highly charged. Thus, they are potentially able to interact with charge groups of the lipid molecules and water. To examine this possibility, we calculated the radial distribution function, $g(r)$, for OL atoms relative to the positively charged choline methyl groups and water oxygen atoms. The RDF describes the probability of finding a particle β at a distance between r and $r + dr$ away from a particle α in a simulation box of volume V containing N particles:

$$\mathrm{RDF} = \frac{V}{N}\left\langle \frac{n(r)}{4\pi r^2\, dr} \right\rangle$$

where $n(r)$ is the number of particles β in a spherical ring of radius r and width dr around the particle α, $4\pi r^2\, dr$ is the ring volume, and $\langle\ \rangle$ denotes an ensemble average. These functions are shown in Figure 10. That figure demonstrates that there are interactions between choline methyl groups and label oxygen

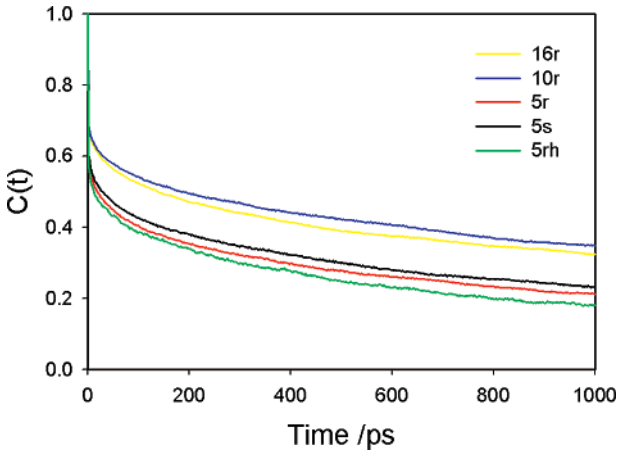

Figure 11. Autocorrelation function representing the presence of charge pairs between SASL OL oxygen atoms and choline methyl groups.

atoms which are documented by the presence of a strong peak at 0.3 nm and a minimum at 0.45 nm. Similar interactions, known as charge pairs, were previously observed between the choline methyl groups and lipid oxygens.[38]

In additional analyses, to define the presence of a charge pair, we used a simple distance criterion where a pair was recorded if the distance between the OL and the choline methyl group was less than the position of the first minimum at $g(r)$. On average, 23% of 10r and 16r, 16% of 5r, 14% of 5s, and 6% of 5rh molecules were involved in this type of interaction. To describe the dynamics of charge pairs, we calculated the time autocorrelation function:

$$\mathrm{ACF}(t) = \langle hw(0)hw(t)\rangle/\langle hw\rangle$$

The function $hw(t)$ adopts a value of 1 if a pair exists and a value of 0 if a pair is broken assuming that a pair exists at time $t = 0$. In this analysis, we follow the approach of Balasubramanian et al. for the dynamics of hydrogen bonding.[39] These autocorrelation functions are shown in Figure 11. The pairs between lipids and 10r or 16r labels are more stable than between lipids and 5r, 5s, or 5rh labels.

As can be seen from Figure 10b, interactions with water are also possible. The small peak at a distance of 0.27 nm indicates the formation of hydrogen bonds with water. However, these are not numerous, and less than 1−2% of the labels can bind with water. Similar analysis of label NL atoms, which are positively charged, did not show specific interactions with water or negatively charged lipid oxygen atoms (data not shown). This is likely to be due to the reduced accessibility of NL, which is more buried among other label ring atoms.

Discussion

In these studies MD simulations of five lipid bilayers with stearic acid spin labels were performed. We studied the effect of label position along the stearyl chain, the effect of chirality at the atom where label is attached, and the effect of label ionization (thus indirectly the effect of pH). First, we noticed that incorporation of SASL molecules into the lipid bilayer results only in a small increase in order parameters and a related decrease of surface area, but it does not change the overall bilayer structure. For comparison, we considered cholesterol, which is the crucial molecule responsible for regulating properties of animal membranes. At 12 mol % concentration, cholesterol was shown to increase twice the membrane order in equivalent MD studies.[40] These small changes in bilayer

properties agree with experimental observations for SASL molecules with respect to the temperature of the main phase transition.[4] The concentration used in this study, 11 mol %, is somewhat high compared to the 1 mol % used in experimental studies. Therefore, the use of SASL in experimental studies seems to be reasonable.

Probably the most important data provided in these studies relate to the position of the label in the membrane and its distribution. The assumption that the SASL molecules labeled at different positions report information on bilayer properties at different depths is important for the interpretation of experimental data. The previous indirect evidence that this is the case comes from the measurements of molecular collision rates between probes labeled at different depths.[11−13] Our data shows clearly and explicitly that, on average, labeled fragments are located at specific membrane depths. The position of the label is shifted compared to the location of acyl tail carbon atoms by two to eight positions depending on the label position. Labels located at the beginning of the tail are less shifted than labels located at the end of the tail. This difference seems to be related to the electrostatic interactions in the interface−SASL molecules labeled deeper are more flexible and more easily interact with choline groups.

When the fifth carbon is labeled, it is difficult for the label to fold back and allow the nitroxide to interact with the water interface. In the case of 10r and 16r, where the chain available for this type of folding is longer, these types of folded conformations are more easily accomplished. Such conformations are visible in the snapshots that are shown in Figure 4b. This is reflected in the number of nitroxide−choline interactions for 10-SASL and 16-SASL with respect to the number for 5-SASL despite the average location of the label being closer to the interface in the latter case. These interactions seem even to stabilize this arrangement. This is very important for EPR spectroscopy. The three probes are located at the different depths, characterized by different mobilities, reflecting the different membrane compartments that they probe.

The width of the vertical position of the label observed in our simulations is 0.25−0.35 nm. This is close to neutron diffraction data which shows that the width of the distribution of the positions of the carbon atoms in the acyl chain is 0.15 nm for the C-4 position and moving to 0.34 nm for the C-12 position.[41] Also, the measurement of the molecular collision rate indicates that distributions of the labeled position are of a similar order.[11−13] It was possible to observe collisions between labels at the 5- and 16-carbon.

An interesting problem, not previously considered, is the potential effect of the chirality of the SASL molecule to the atom to which the label is attached. In this study, we considered two chiral forms of the 5-SASL molecule. We chose this probe due to its location in the more rigid region of hydrocarbon core closer to the interface where we expect that the difference in chirality may play a role. At this point, we should stress the lack of any information on chirality of commercially available probes. Therefore, it is likely that they consist of a racemic mixture of both forms. Results obtained in our simulations show almost identical rotation of the N−O bond in the short time scale (see inset to Figure 8) for both chiral forms, with their location in the membrane being slightly different. The *S* form is located about 0.2 nm deeper in the membrane core. This is associated with slightly fewer charge pairs between the probe and choline methyl groups. These results do not allow us to strongly conclude if the chirality of the probe can be important from the point of view of EPR spectroscopy or not. Small effects of chirality on spectroscopic results cannot be excluded. This issue should be the subject of future experimental work.

In experimental conditions, the carboxyl acid group of the SASL molecule should be in a dissociated charge form. This is ensured by using the appropriate buffer condition and a rather high pH of 9.5,[2−4] since the carboxyl group of 5-SASL in the membrane showed an apparent pK_a of around 7.5.[42] The effect of pH on EPR spectra of SASLs was investigated previously. It was shown that pH titration curves were affected by the headgroup structure, acyl chain length, and the location of spin labels on the stearic acid chain.[42] The effects were mainly caused by a change in the vertical location of spin labels in the membrane due to the protonation of the carboxyl group and the hydrophilic character of the nitroxide group of spin labels. Simulations of charged and uncharged SASL molecules mimic the effect of pH on SASL behavior. As can be seen, the uncharged form of SASL behaves drastically differently from that of charged SASL molecules. It is located deeper in the membrane and is able to diffuse between membrane layers during the simulation time, and its rotation seems to be almost isotropic. It should be stressed that this is, to the best of our knowledge, the second time in MD simulations when spontaneous diffusion of molecules between two membrane layers has been observed. The first time, we observed flip-flop diffusion in MD simulations of ketosterol-containing bilayers (cholesterol molecule with a ketone instead of hydroxyl headgroup).[43]

Acknowledgment. Tomasz Róg holds a Marie Curie Intra-European Fellowship "024612-Glychol". Computational resources were provided by the Barcelona Supercomputing Center and the SharcNet grid computing facility (www.sharcnet.ca). We thank the Academy of Finland, the Emil Aaltonen Foundation, and the Natural Sciences and Engineering Research Council of Canada (NSERC) for financial support.

References and Notes

(1) Hubbell, W. L.; McConnell, H. M. *J. Am. Chem. Soc.* **1971**, *93*, 314−326.
(2) Subczynski, W. K.; Hyde, J. S.; Kusumi, A. *Proc. Natl. Acad. Sci. U.S.A.* **1989**, *86*, 4474−4478.
(3) Subczynski, W. K.; Wisniewska, A.; Yin, J.-J.; Hyde, J. S.; Kusumi, A. *Biochemistry* **1994**, *33*, 7670−7681.
(4) Wisniewska, A.; Nishimoto, Y.; Hyde, J. S.; Kusumi, A.; Subczynski, W. K. *Biochim. Biophys. Acta* **1996**, *1278*, 68−72.
(5) Ge, M.; Freed, J. H. *Biophys. J.* **1998**, *74*, 910−917.
(6) Marsh, D. Electron Spin Resonance: Spin Labels. In *Membrane Spectroscopy*; Grell, E., Ed.; Springer-Verlag, New York, 1981.
(7) Subczynski, W. K.; Hyde, J. S.; Kusumi, A. *Biochemistry* **1991**, *30*, 8578−8590.
(8) Subczynski, W. K.; Wisniewska, A.; Hyde, J. S.; Kusumi, A. *Biophys. J.* **2007**, *92*, 1573−1584.
(9) Pace, R. J.; Chan, S. I. *J. Chem. Phys.* **1982**, *76*, 4241−4247.
(10) Altenbach, C.; Greenhalgh, D. A.; Khorana, H. G.; Hubbell, W. L. *Proc. Natl. Acad. Sci. U.S.A.* **1994**, *91*, 1667−1671.
(11) Yin, J.-J.; Feix, J. B.; Hyde, J. S. *Biophys. J.* **1990**, *58*, 713−720.
(12) Yin, J.-J.; Subczynski, W. K. *Biophys. J.* **1996**, *71*, 832−839.
(13) Merkle, H.; Subczynski, W. K.; Kusymi, A. *Biochim. Biophys. Acta* **1987**, *897*, 238−248.
(14) Mravljak, J.; Konc, J.; Hodoscek, M.; Solmajer, T.; Pecar, S. *J. Phys. Chem. B* **2006**, *110*, 25559−25561.
(15) Murzyn, K.; Róg, T.; Blicharski, W.; Dutka, M.; Pyka, J.; Szytula, S.; Froncisz, W. *Proteins* **2006**, *62*, 1088−1100.
(16) Steinhoff, H. J.; Müller, M.; Beier, C.; Pfeiffer, M. *J. Mol. Liq.* **2000**, *84*, 17−27.
(17) LaConte, L. E. W.; Voelz, V.; Nelson, W.; Enz, M.; Thomas, D. D. *Biophys. J.* **2002**, *83*, 1854−1866.
(18) Håkansson, P.; Westlund, P. O.; Lindahl, E.; Edholm, O. *Phys. Chem. Chem. Phys.* **2001**, *3*, 5311−5319.
(19) Sammalkorpi, M.; Lazaridis, T. *Biophys. J.* **2007**, *92*, 10−22.
(20) Róg, T.; Murzyn, K.; Gurbiel, R.; Takaoka, Y.; Kusumi, A.; Pasenkiewicz-Gierula, M. *J. Lipid Res.* **2004**, *45*, 326−336.

(21) Patra, M.; Karttunen, M.; Hyvönen, M. T.; Lindqvist, P.; Falck, E.; Vattulainen, I. *Biophys. J.* **2003**, *84*, 3636−3645.
(22) Lindahl, E.; Hess, B.; van der Spoel, D. *J. Mol. Model*. **2001**, *7*, 306−317.
(23) Róg, T.; Vattulainen, I.; Pasenkiewicz-Gierula, M.; Karttunen, M. *Biophys. J*. **2007**, *92*, 3346−3357.
(24) Aittoniemi, J.; Róg, T.; Niemelä, P.; Pasenkiewicz-Gierula, M.; Karttunen, M.; Vattulainen, I. *J. Phys. Chem. B* **2006**, *110*, 25562−25564.
(25) Berger, O.; Edholm, O.; Jahnig, F. *Biophys. J*. **1997**, *72*, 2002−2013.
(26) Tieleman, D. P.; Berendsen, H. J. C. *J. Chem. Phys*. **1996**, *105*, 4871−4880.
(27) Berendsen, H. J. C.; Postma, J. P. M.; van Gunsteren, W. F.; Hermans, J. Interaction models for water in relation to protein hydration. In *Intermolecular Forces.* Pullman, B., Ed.; Reidel: Dordrecht, The Netherlands, 1981.
(28) Patra, M.; Karttunen, M. *J. Comput. Chem.* **2004**, *25*, 678−689.
(29) Improta, R.; Di Matteo, A.; Barone, V. *Theor. Chem. Acc*. **2000**, *104*, 273−279.
(30) Hess, B.; Bekker, H.; Berendsen, H. J. C.; Fraaije, J. G. E. M. *J. Comput. Chem*. **1997**, *18*, 1463−1472.
(31) Berendsen, H. J. C.; Postma, J. P. M.; van Gunsteren, W. F.; DiNola, A.; Haak, J. R. *J. Chem. Phys.* **1984**, *81*, 3684−3690.
(32) Vist, M. R.; Davis, J. H. *Biochemistry* **1990**, *29*, 451−464.
(33) Essman, U.; Perera, L.; Berkowitz, M. L.; Darden, T.; Pedersen, L. G. *J. Chem. Phys.* **1995**, *103*, 8577−8592.
(34) Patra, M.; Karttunen, M.; Hyvönen, M. T.; Falck, E.; Vattulainen, I. *J. Phys. Chem. B* **2004**, *108*, 4485−4494.
(35) Hess, B. *J. Chem. Phys*. **2002**, *116*, 209−217.
(36) Davis, J. H. *Biochim. Biophys. Acta* **1983**, *737*, 117−171.
(37) Gaffney, B. J.; Marsh, D. *Proc. Natl. Acad. Sci. U.S.A.* **1998**, *95*, 12940−12943.
(38) Murzyn, K.; Róg, T.; Jezierski, G.; Takaoka, Y.; Pasenkiewicz-Gierula, M. *Biophys. J.* **2001**, *81*, 170−183.
(39) Balasubramanian, S.; Pal, S.; Bagchi, B. *Phys. Rev. Lett*. **2002**, *89*, 115505.
(40) Falck, E.; Patra, M.; Karttunen, M.; Hyvönen, M. T.; Vattulainen, I. *Biophys. J*. **2004**, *87*, 1076−1091.
(41) Zaccai, G.; Büldt, G.; Seelig, A.; Seelig, J. *J. Mol. Biol*. **1979**, *134*, 693−706.
(42) Kusumi, A.; Subczynski, W. K.; Hyde, J. S. *Fed. Proc*. **1982**, *41*, 1394, abst 6671.
(43) Róg, T.; Stimson, L. M.; Pasenkiewicz-Gierula, M.; Vattulainen I.; Karttunen M. Replacing the cholesterol hydroxyl group by the ketone group facilitates sterol flip-flop and promotes membrane fluidity. In press.